ing, and smooth muscle cell hyperplasia in atherosclerosis (*3, 4*). These proliferative events have been ascribed mostly to macrophage-derived PDGF, a potent fibroblast and smooth muscle cell mitogen (*4*). Macrophage-derived HB-EGF could be equally important in these processes. Since HB-EGF is also mitogenic for keratinocytes (*17*), it could, unlike EGF and PDGF, have a dual role in wound healing by stimulating epithelialization after injury as well as connective tissue growth. In addition, as postulated for other heparin-binding growth factors (*18*), the ability of HB-EGF to stimulate cell proliferation might be facilitated by a mechanism in which it binds to heparin-like sites on cell surfaces and in extracellular matrix.

REFERENCES AND NOTES

1. C. F. Nathan, *J. Clin. Invest.* **79**, 319 (1987).
2. A. Baird, P. Mormede, P. Bohlen, *Biochem. Biophys. Res. Commun.* **126**, 358 (1985); K. Shimokado *et al.*, *Cell* **43**, 277 (1985); D. K. Madtes *et al.*, *ibid.* **53**, 285 (1988); R. K. Assoian *et al.*, *Proc. Natl. Acad. Sci. U.S.A.* **84**, 6020 (1987); S. J. Leibovich *et al.*, *Nature* **329**, 630 (1988).
3. N. M. Aqel, R. Y. Ball, H. Walsmann, M. J. Mitchinson, *J. Pathol.* **146**, 197 (1985).
4. R. Ross, *N. Engl. J. Med.* **314**, 488 (1986).
5. Y. Shing *et al.*, *Science* **223**, 1296 (1984); M. Klagsbrun and Y. Shing, *Proc. Natl. Acad. Sci. U.S.A.* **82**, 805 (1985); M. Klagsbrun, J. Sasse, R. Sullivan, S. Smith, J. A. Smith, *ibid.* **83**, 2448 (1986).
6. W. H. Burgess and T. Maciag, *Annu. Rev. Biochem.* **58**, 575 (1989).
7. G. Besner, S. Higashiyama, M. Klagsbrun, *Cell Regul.* **1**, 811 (1990).
8. J. O. Minta and L. Pambrun, *Am. J. Pathol.* **119**, 111 (1985).
9. U-937 cells (American Type Culture Collection) were treated with TPA as in Fig. 1A, and adherent cells were then incubated for 24 hours in serum-free RPMI 1640. Conditioned medium (8 liters) was collected and applied to a BioRex 70 (Bio-Rad) cation-exchange column (5 by 10 cm) equilibrated with 0.2 M NaCl and 0.01 M tris-HCl, pH 7.5. Growth factor activity (stimulation of DNA synthesis in BALB-3T3 cells) was batch-eluted with 1 M NaCl and 0.01 M tris-HCl, pH 7.5, at a flow rate of 300 ml/hour. The eluate was adjusted to pH 8.0 and applied to a copper-chelating Sepharose column (2 by 11 cm, Pharmacia LKB Biotechnology) saturated with copper chloride and equilibrated in 0.5 M NaCl and 0.01 M tris-HCl, pH 8.0. The copper-chelating column was washed with a 200-ml linear gradient of 0 to 0.04 M L-histidine, 0.5 M NaCl, and 0.01 M tris-HCl, pH 8.0, at a flow rate of 40 ml/hour. A single peak of growth factor activity eluting at 0.02 to 0.025 M L-histidine was pooled, diluted 1:1 with 0.01 M tris-HCl, pH 7.5, and applied to an FPLC TSK heparin affinity column, as in Fig. 1A. Growth factor eluting at 1 to 1.2 M NaCl was subjected to RP-HPLC on a C_4 column (4.6 by 250 mm, Vydac, Beckman model 334 HPLC system) and eluted with a 0 to 40% gradient of acetonitrile. HB-EGF was purified approximately 7500-fold, the yield was 15%, and about 1.2 μg of HB-EGF was recovered from 8 liters of conditioned medium.
10. Single letter amino acid abbreviations used are as follows: A, Ala; C, Cys; D, Asp; E, Glu; F, Phe; G, Gly; H, His; I, Ile; K, Lys; L, Leu; M, Met; N, Asn; P, Pro; Q, Gln; R, Arg; S, Ser; T, Thr; V, Val; W, Trp; Y, Tyr; and X, no residue detected. The identification of one Lys in the NH_2-terminal sequencing was questionable.
11. J. Devereux, P. Haeberli, O. Smithies, *Nucleic Acids Res.* **12**, 387 (1984); W. R. Pearson and D. J. Lipman, *Proc. Natl. Acad. Sci. U.S.A.* **85**, 2444 (1988).
12. Filter replicas of approximately 1.4×10^6 plaques from a TPA-stimulated U-937 cell cDNA library in λgt10 (Clontech) were screened with a ^{32}P-labeled antisense oligonucleotide probe (5′-CTTG/TCCATGCTCCTCCTTGTTA/GGGCTTGGCCAGGGCCTGA/GGGCTT-3′, where a slash between two bases indicates that either could be used at that position) designed based on amino acids 6 to 20 of the NH_2-terminal HB-EGF sequence. Hybridizations were carried out at 42°C in 20% formamide buffer as described [W. I. Wood *et al.*, *Nature* **312**, 330 (1984)], except that no dextran sulfate was used. The filters were washed at 46°C in 1× saline sodium citrate (0.15 M NaCl, 0.015 M sodium citrate, pH 7.0) containing 0.1% SDS before autoradiography. Fourteen hybridizing clones were purified, and the insert DNA fragments in several of these clones were isolated and subcloned into M13 cloning vectors [J. Vieira and J. Messing, *Methods Enzymol.* **153**, 3 (1987)] for sequencing by the dideoxy technique [F. Sanger, A. R. Coulson, B. G. Barrell, A. J. H. Smith, B. A. Roe, *J. Mol. Biol.* **143**, 161 (1980)].
13. G. von Heijne, *Eur. J. Biochem.* **133**, 17 (1983).
14. H. Gregory, *Nature* **257**, 235 (1975).
15. R. Derynck, A. B. Roberts, M. E. Winkler, E. Y. Chen, D. V. Goeddel, *Cell* **38**, 287 (1984).
16. M. Shoyab, V. L. McDonald, J. G. Bradley, G. J. Todaro, *Proc. Natl. Acad. Sci. U.S.A.* **85**, 6528 (1988); M. Shoyab, G. D. Plowman, V. L. McDonald, J. G. Bradley, G. J. Todaro, *Science* **243**, 1074 (1989); G. Plowman *et al.*, *Mol. Cell. Biol.* **10**, 1969 (1990).
17. S. Higashiyama and M. Klagsbrun, unpublished observations.
18. D. Moscatelli, *J. Cell. Physiol.* **131**, 123 (1987); A. Baird and N. Ling, *Biochem. Biophys. Res. Commun.* **142**, 428 (1987); I. Vlodavsky *et al.*, *Proc. Natl. Acad. Sci. U.S.A.* **84**, 2292 (1987); M. Y. Gordon, G. P. Riley, S. M. Watt, M. F. Greaves, *Nature* **326**, 403 (1987); R. Roberts *et al.*, *ibid.* **332**, 376 (1988).
19. N. Iberg, S. Rogelj, P. Fanning, M. Klagsbrun, *J. Biol. Chem.* **264**, 19951 (1989).
20. U. K. Laemmli, *Nature* **277**, 680 (1970); B. R. Oakley, D. R. Kirsch, N. R. Morris, *Anal. Biochem.* **105**, 361 (1980).
21. R. N. Fabricant, J. E. DeLarco, G. J. Todaro, *Proc. Natl. Acad. Sci. U.S.A.* **74**, 565 (1977); H. Haigler, J. F. Ash, S. J. Singer, S. Cohen, *ibid.* **75**, 3317 (1978).
22. E. S. Kimball and T. C. Warren, *Biochim. Biophys. Acta* **771**, 82 (1984); J. Singh, *Methods Enzymol.* **147**, 13 (1987).
23. H. Lehrach, D. Diamond, J. M. Wozney, H. Boedtker, *Biochemistry* **16**, 4743 (1977).

24. Supported in part by NIH grants CA37392 and CA45548 (M.K.). We thank R. Mitchell for help with RNA analysis, J. Iwasa for oligonucleotide synthesis, S. Moskowitz and E. Stoelting for preparation of the figures, and M. Vultaggio for preparation of the manuscript. Microsequencing was carried out by W. Lane (Harvard BioLabs).

14 September 1990; accepted 27 November 1990

Mutations Affecting Internal TEA Blockade Identify the Probable Pore-Forming Region of a K^+ Channel

GARY YELLEN, MARK E. JURMAN, TATIANA ABRAMSON, RODERICK MACKINNON

The active site of voltage-activated potassium channels is a transmembrane aqueous pore that permits ions to permeate the cell membrane in a rapid yet highly selective manner. A useful probe for the pore of potassium-selective channels is the organic ion tetraethylammonium (TEA), which binds with millimolar affinity to the intracellular opening of the pore and blocks potassium current. In the potassium channel encoded by the *Drosophila Shaker* gene, an amino acid residue that specifically affects the affinity for intracellular TEA has now been identified by site-directed mutagenesis. This residue is in the middle of a conserved stretch of 18 amino acids that separates two locations that are both near the external opening of the pore. These findings suggest that this conserved region is intimately involved in the formation of the ion conduction pore of voltage-activated potassium channels. Further, a stretch of only eight amino acid residues must traverse 80 percent of the transmembrane electric potential difference.

TO UNDERSTAND THE MOLECULAR mechanisms of ion conduction and selectivity in voltage-activated potassium channels, we must first identify the specific parts of the channel protein that line the pore. Potassium channels are multimeric proteins; each of the subunits probably contributes to the lining of a central pore (*1*). Although several models for the transmembrane folding of a K^+ channel subunit have been proposed (*2–6*), it is unclear what region of the protein actually lines the aqueous pore. Several amino acid residues are known to lie in the external mouth of the pore (*5–7*). We set out to identify residues at the inner mouth of the pore in order to define the topology of the pore forming region of the protein and thus to indicate the residues that may line the ion conduction pathway.

Internal application of TEA prevents the

G. Yellen and M. E. Jurman, Howard Hughes Medical Institute and the Departments of Neuroscience and Biophysics and Biophysical Chemistry, The Johns Hopkins University School of Medicine, Baltimore, MD 21205.
T. Abramson, and R. MacKinnon Department of Cellular and Molecular Physiology, Harvard Medical School, Boston, MA 02115.

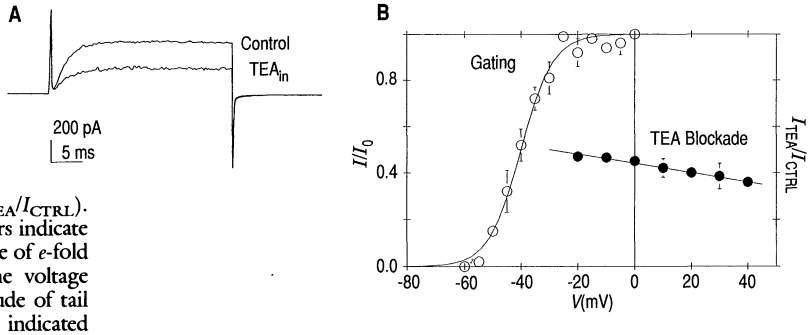

Fig. 1. Intracellular TEA blockade of the ShIR channel. (**A**) The effect of internal TEA (1 mM) on K^+ currents evoked by a voltage-clamp pulse from −80 to 0 mV. An inside-out patch from an oocyte injected 48 hours previously with RNA coding for the wild-type ShIR channel (*15, 23*) was exposed to control saline or to saline containing 1 mM TEACl. (**B**) Voltage dependence of TEA blockade compared with the voltage dependence of gating. TEA blockade is the ratio of the steady-state current in the presence and absence of 1 mM internal TEA (I_{TEA}/I_{CTRL}). Each point is the average of two to four determinations; error bars indicate range or SEM. The solid line corresponds to a voltage dependence of *e*-fold per 160 mV or an equivalent electrical distance of 0.15. The voltage dependence of gating was determined by measuring the amplitude of tail currents at −120 mV after a 30-ms depolarizing pulse to the indicated voltage. These amplitudes are normalized (I/I_0) so that the value for a pulse to 0 mV is unity. Each point is the average of five to eight determinations; error bars indicate SEM. The smooth line is a Boltzmann distribution with a midpoint at −40 mV and a slope of *e*-fold per 5.7 mV. The external (pipette) solution contained 155 mM NaCl, 5 mM KCl, 3 mM $CaCl_2$, 1 mM $MgCl_2$, 10 mM Hepes (pH 7.4); the internal (bath) solution contained 160 mM KCl, 1 mM EGTA, 0.5 mM $MgCl_2$, 10 mM Hepes (pH 7.4).

conduction of K^+ ions through voltage-activated K^+ channels (*8–10*). Several pieces of evidence indicate that internal TEA acts by plugging the pore. First, TEA gains access to the internal binding site only when the voltage-dependent activation gate of the channel is open (*11*). Second, when the gate is open, blockade by TEA is sensitive to the transmembrane voltage in a fashion consistent with the partial penetration of TEA into the pore (*9, 12, 13*). Finally, dissociation of TEA analogs is enhanced by a high concentration of K^+ on the opposite (external) side of the channel, as though K^+ can enter the pore from the opposite side and expel the TEA analog (*14*). Therefore, TEA is a good probe of the internal entryway to the ion conduction pore of K^+ channels.

We investigated the action of internal TEA on the Shaker K^+ channel. To study TEA blockade of the open channel without interference from gating, we used a mutant (*ShIR*) that does not inactivate during short depolarizations (*15*). Internal TEA blocks the ShIR K^+ channel with submillimolar affinity (Fig. 1A). The blockade is weakly voltage dependent (Fig. 1B), a result consistent with a TEA inhibition site located 15% of the way into the transmembrane electric field (*12, 13*). We measured the blocking properties at voltages that fully activate the channel (see gating curve in Fig. 1B), thus avoiding interference from activation gating.

We prepared several mutations of the ShIR channel that introduce conservative amino acid changes in the SS1-SS2 region of the channel, which is located between the S5 and S6 putative membrane spanning sequences [(*16*) see Fig. 4]. Several residues flanking the SS1-SS2 region lie in the outer mouth of the pore, as shown by their influence on external charybdotoxin blockade, external TEA blockade, and ion permeation (*5–7*). The SS1-SS2 region itself is conserved among voltage-activated K^+ channels and has been proposed to cross the membrane twice and form the ion conductive pore (*4–6*). This hypothesis predicts that some part of the SS1-SS2 region may extend to the internal entryway of the pore, and thus mutations in this region may affect internal TEA blockade. We mutated each of the threonine residues in the middle of the SS1-SS2 region—at positions 439, 441, and 442—to serine. The T442S mutant channel exhibited abnormal gating, which made it unsuitable for study (*17*). The T439S mutation had wild type sensitivity to internal TEA (see Fig. 4A). In contrast, the mutation at position 441 exhibited dramatically altered sensitivity to internal TEA. The T441S mutant channel was ten times less sensitive to TEA than was the wild type ShIR channel (Fig. 2A). This result is in agreement with the idea that this region spans the membrane twice.

The T441S mutation appears to affect internal TEA blockade specifically, since many other properties of the channel remain unaltered. The mutant channel had wild type sensitivity to external TEA (Fig. 2B). Activation gating of the mutant was also normal (Fig. 3A). Introduction of the T441S mutation into the Shaker H4 channel, which inactivates rapidly, did not affect the rapid inactivation gating process (Fig. 3B). The single channel conductance and the extrapolated reversal potential in physiological solutions were unaltered (Fig. 3C).

We next tested whether the mutations that alter external TEA blockade (*5*) also affect internal TEA blockade, and vice versa. We had already observed that the T441S mutation left the sensitivity of the ShIR channel to external TEA unaltered (Fig. 2B). Two mutants that significantly alter external TEA sensitivity, D431K and T449Y, had completely normal sensitivity to internal TEA block (Fig. 4A). These findings indicate that the external and the internal TEA binding sites are separate, as expected from their distinct physiological properties (*10, 18*).

Several lines of evidence indicate that the regions flanking the SS1-SS2 are located externally. First, the interaction of the channel with charybdotoxin, which blocks the external mouth of the pore, is influenced by mutations in these regions (*6, 7*). Some of these mutations influence toxin binding by

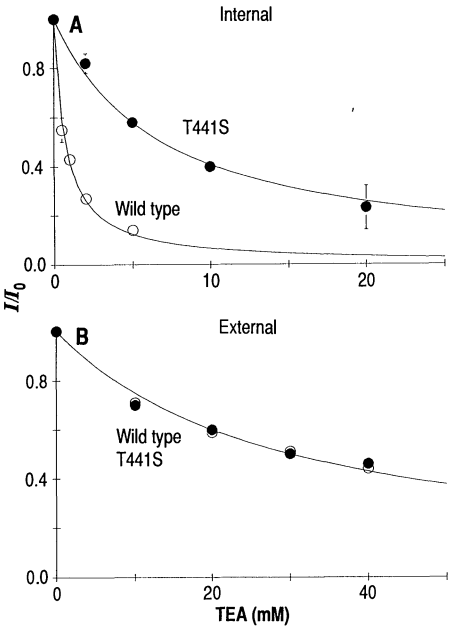

Fig. 2. The TEA sensitivity of the T441S mutant. (**A**) Internal TEA blockade. The fractional reduction in steady-state outward current at 0 mV (I/I_0) as a function of internal TEA concentration for the ShIR channel and the T441S mutant of ShIR. Measurements were made on excised inside-out patches as for Fig. 1. Each point is the average of three to seven determinations; error bars indicate SEM. (**B**) External TEA blockade. The fractional reduction in steady-state outward current at 0 mV (I/I_0) as a function of external TEA concentration. Each point is the average of three to five determinations; error bars indicate SEM. Measurements were made with a two-microelectrode voltage clamp of injected oocytes, as in (*6*). The recording saline contained 96 mM NaCl, 2 mM KCl, 0.3 mM $CaCl_2$, 1 mM $MgCl_2$, 5 mM Hepes (pH 7.6); TEACl was substituted for an equivalent amount of NaCl.

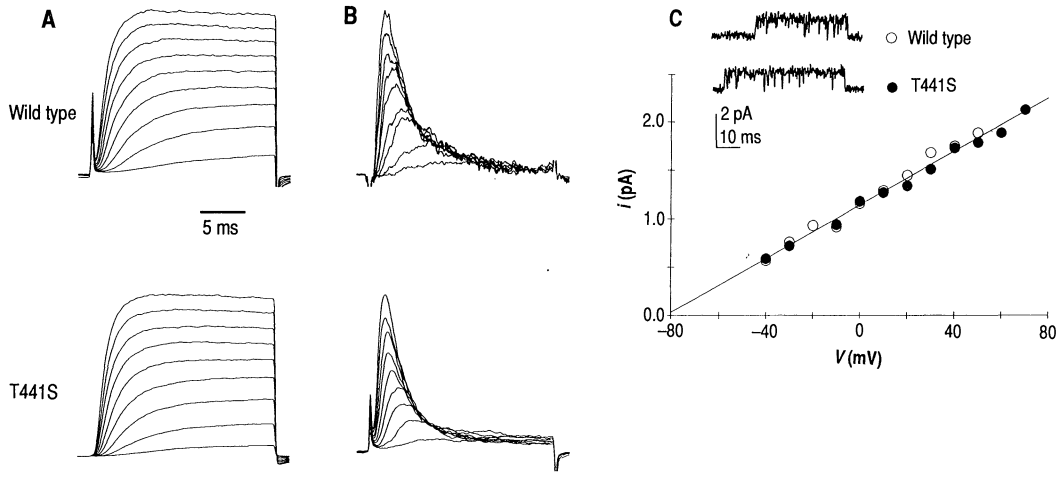

Fig. 3. Gating and single channel behavior of the T441S mutant channel. (**A**) Voltage activation of ShIR (upper) and T441S (ShIR) (lower). (**B**) Voltage activation of Shaker H4 (upper) and T441S (in Shaker H4) (lower). Macroscopic currents through many channels were recorded from inside-out patches from oocytes injected with the indicated RNA. Outward K^+ currents were evoked by a series of depolarizing voltage steps to between −40 and +40 mV in 10-mV increments; the holding potential was −80 mV and the pulse duration was 20 ms. Conditions as in Fig. 1A. Maximum currents are (A) upper, 5.1 nA; (A) lower, 8.8 nA; (B) upper, 0.29 nA; (B) lower, 0.79 nA. (**C**) Unitary current (*i*)–voltage (*V*) relation for ShIR and T441S (ShIR) channels. Unitary currents were measured from records like those in the inset. The silent periods before and after the openings probably correspond to the slow inactivated state; brief pulses to 0 from −80 mV seldom resulted in long closures. Recordings were from inside-out patches, as in Fig. 1A, but contained fewer channels. The solid line corresponds to a slope conductance of 13 pS with an extrapolated reversal potential of −82 mV. The calculated equilibrium potential for K^+ was −87 mV.

an electrostatic and thus local mechanism. Second, external TEA blockade is affected by mutations at the 431 and 449 positions. The 449 position is especially critical in determining external TEA sensitivity; substitution of different amino acids at this position results in inhibition constants that vary over a 500-fold range (*5*).

Amino acid residue 441 is in the middle of the SS1-SS2 region, and it interacts with internal TEA. Together with the external location of the flanking regions, these data indicate that the SS1-SS2 region most likely crosses the membrane twice (Fig. 4B). This conclusion means that a remarkably short stretch of eight amino acids (441 to 449) connects the two ends of the pore, since TEA blocks superficially from both sides. From the inside, TEA traverses only 15% of the transmembrane electric potential to reach its binding site (Fig. 1B). From the outside, TEA traverses only 5% of the potential (*19*). Thus, 80% of the transmembrane electric potential falls across the eight amino acids between residues 441 and 449. This chain length is much shorter than that usually postulated for α-helical membrane-spanning regions (*20*); an α-helix containing eight amino acids has a length of only 12 Å. It is possible that the SS1-SS2 region does not span the entire thickness of the membrane in which case the channel would have an hourglass-like structure, with a short narrow pore and wider vestibules at one or both ends. An alternative hypothesis, which is more compatible with the propensity of voltage-activated K^+ channels to accommodate multiple K^+ ions simultaneously (*21*), is that the SS1-SS2 region adopts a more extended β conformation. A β-strand of eight amino acids has a length of about 27 Å (approximately the same length as a 20–amino acid α-helix). This is nearly the estimated length (30 Å) of the pore of a different K^+ channel, the large-conductance Ca^{2+}-activated K^+ channel (*22*).

Our mutagenesis experiments on the Shaker K^+ channel provide evidence that the SS1-SS2 region crosses the membrane twice and is intimately associated with the ion conduction pore.

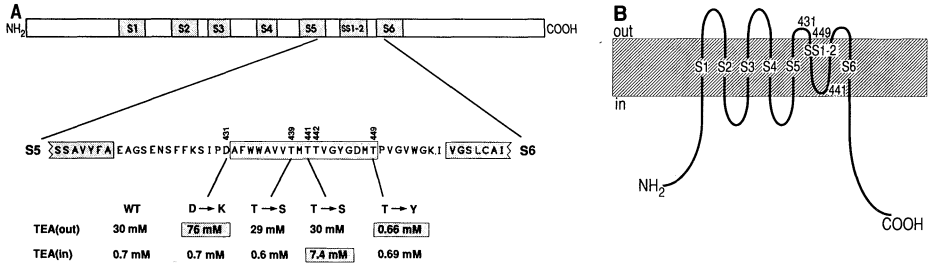

Fig. 4. (**A**) Amino acid sequence of the SS1-SS2 region of the ShIR channel and the effects of mutations on inhibition by external and internal TEA. S1 to S6 are hydrophobic regions of the Shaker protein thought to span the membrane (*2, 3*). The SS1-SS2 region is the central boxed portion of the sequence, from positions 432 through 449 (*15*). The inhibition constants for external and internal TEA blockade (determined as in Fig. 2) are indicated for the wild-type ShIR channel and for each mutant. Each value is an average of multiple determinations on three to ten patches; all SEMs are less than 15% of the value shown. The values that differ significantly from those of the wild-type channel are boxed. (**B**) Transmembrane topology model for the Shaker K^+ channel based on previous predictions and on the data in this report. The amino acids are abbreviated as follows: A, alanine; C, cysteine; D, aspartate; E, glutamate; F, phenylalanine; G, glycine; H, histidine; I, isoleucine; K, lysine; L, leucine; M, methionine; N, asparagine; P, proline; Q, glutamine; R, arginine; S, serine; T, threonine; V, valine; W, tryptophan; and Y, tyrosine.

REFERENCES AND NOTES

1. M. J. Christie, R. A. North, P. B. Osborne, J. Douglass, J. P. Adelman, *Neuron* **4**, 405 (1990); E. Y. Isacoff, Y. N. Jan, L. Y. Jan, *Nature* **345**, 530 (1990); J. P. Ruppersberg *et al.*, *ibid.*, p. 535; R. MacKinnon, *ibid.*, in press.
2. B. L. Tempel, D. M. Papazian, T. L. Schwarz, Y. N. Jan, L. Y. Jan, *Science* **237**, 770 (1987).
3. W. A. Catterall, *ibid.* **242**, 50 (1988).
4. H. R. Guy, in *Monovalent Cations in Biological Systems*, C. A. Pasternak, Ed. (CRC Press, Cleveland, OH, 1989).
5. R. MacKinnon and G. Yellen, *Science* **250**, 276 (1990).
6. R. MacKinnon, L. Heginbotham, T. Abramson, *Neuron* **5**, 767 (1990).
7. R. MacKinnon and C. Miller, *Science* **245**, 1382 (1989).
8. I. Tasaki and S. Hagiwara, *J. Gen. Physiol.* **40**, 859 (1957); E. Koppenhoefer and W. Vogel, *Pfluegers Arch.* **313**, 361 (1969).
9. C. M. Armstrong and L. Binstock, *J. Gen. Physiol.* **48**, 859 (1965).
10. C. M. Armstrong and B. Hille, *ibid.* **59**, 388 (1972).
11. C. M. Armstrong, *ibid.* **50**, 491 (1966).
12. A. M. Woodhull, *ibid.* **61**, 687 (1973).
13. R. J. French and J. J. Shoukimas, *Biophys. J.* **34**, 271 (1981).
14. C. M. Armstrong, *J. Gen. Physiol.* **54**, 553 (1969); *ibid.* **58**, 413 (1971).
15. The ShIR channel is a mutant of the Shaker H4 channel with an NH_2-terminal deletion; the deletion removes amino acids 6 to 46 of the Shaker H4 protein and results in the abolition of rapid inactivation, as reported for the Shaker B channel [T. Hoshi, W. N. Zagotta, R. W. Aldrich, *Science* **250**, 533 (1990)]. The positions of all of the mutations made in this paper refer to the original numbering of the Shaker H4 sequence [A. Kamb, J. Tseng-Crank, M. A. Tanouye, *Neuron* **1**, 421 (1988)] which is nearly identical to the Shaker B sequence (*2*).
16. The SS1-SS2 region is sometimes called H5 (*2*).
17. T442S mutant channels exhibit altered voltage and

time dependence of activation and require prolonged periods (minutes) for recovery between depolarizing steps.
18. P. R. Stanfield, *Rev. Physiol. Biochem. Pharmacol.* **97**, 1 (1983); G. Yellen, *Annu. Rev. Biophys. Biophys. Chem.* **16**, 227 (1987).
19. R. MacKinnon and G. Yellen, unpublished data.
20. L. Stryer, *Biochemistry* (Freeman, New York, ed. 3, 1988).
21. A. L. Hodgkin and R. D. Keynes, *J. Physiol. (London)* **128**, 61 (1955); P. Horowicz, P. W. Gage, R. S. Eisenberg, *J. Gen. Physiol.* **51**, 193s (1968); B. Hille and W. Schwarz, *ibid.* **72**, 409 (1978); T. B. Begenisich and P. DeWeer, *ibid.* **76**, 83 (1980); B. C. Spalding, O. Senyk, J. G. Swift, P. Horowicz, *Am. J. Physiol.* **241**, c68 (1981).
22. Experiments with bis-quaternary ammonium blockers [A. Villarroel, O. Alvarez, A. Oberhauser, R. Latorre, *Pfluegers Arch.* **413**, 118 (1988)] indicate that 27% of the electric potential falls across a physical distance of about 10 Å. If the potential falls linearly over the narrow region of the pore, then 80% of the potential would fall across a distance of about 30 Å.
23. Mutagenesis, RNA synthesis, oocyte injection, voltage-clamp and patch-clamp methods are as described [R. MacKinnon, P. Reinhart, M. M. White, *Neuron* **1**, 997 (1988); (*5*)].
24. We thank L. Heginbotham and P. Hess for helpful comments on the manuscript. G.Y. is a Howard Hughes Medical Institute investigator. R.M. was supported by NIH research grant GM4399.

21 November 1990; accepted 18 January 1991

Exchange of Conduction Pathways Between Two Related K^+ Channels

HALI A. HARTMANN, GLENN E. KIRSCH, JOHN A. DREWE, MAURIZIO TAGLIALATELA, ROLF H. JOHO, ARTHUR M. BROWN

The structure of the ion conduction pathway or pore of voltage-gated ion channels is unknown, although the linker between the membrane spanning segments S5 and S6 has been suggested to form part of the pore in potassium channels. To test whether this region controls potassium channel conduction, a 21–amino acid segment of the S5-S6 linker was transplanted from the voltage-activated potassium channel NGK2 to another potassium channel DRK1, which has very different pore properties. In the resulting chimeric channel, the single channel conductance and blockade by external and internal tetraethylammonium (TEA) ion were characteristic of the donor NGK2 channel. Thus, this 21–amino acid segment controls the essential biophysical properties of the pore and may form the conduction pathway of these potassium channels.

VOLTAGE-GATED ION CHANNELS are thought to consist of four similar domains forming a central pore (*1–4*) with each repeat consisting of six transmembrane segments, S1 to S6 (Fig. 1A). The linker region connecting S5 and S6 is highly conserved, especially in K^+ channels, and therefore seemed a candidate for the conduction pathway of K^+ channels (*2, 3, 5, 6*). In support of this notion is evidence that point mutations in the S5-S6 loop of the Shaker K^+ channel (*7, 8*) changed the blockade produced by a large peptide toxin charybdotoxin (7) and the small, open channel blocker TEA (*8, 9*), and also changed single channel conductance (*8*). To test the role of the S5-S6 linker in forming the channel pore we took advantage of the differences in pore properties of two related K^+ channels DRK1 (*10*) and NGK2 (*11*). The single channel conductance of NGK2 is almost three times that of DRK1, and NGK2 was more sensitive to blockade by TEA applied to the external side of the membrane whereas DRK1 was more sensitive to blockade by TEA applied to the internal side of the membrane. We attempted to modify these properties of the channel by exchanging the S5-S6 loop between the two K^+ channels. To do this, we introduced silent restriction endonuclease sites into DRK1, which allowed removal of a 21–amino acid segment in the S5-S6 linker region, and then generated a chimeric channel in which the corresponding segment was transferred from NGK2 to DRK1 (Fig. 1B) (*12*). If this segment constituted the pore, our prediction was that the chimeric channel should have the conductance and TEA blocking profile of the donor NGK2 channel.

When the chimeric DRK-NGK channel was expressed in oocytes (*13*) the unitary currents at a test potential of 0 mV were about three times greater than those of DRK1 (Fig. 2A). The slope conductance measured over the test potential range of −10 to +40 mV was also about three times greater than that of DRK1 (Fig. 2B). At test potentials outside this range, some curvature was apparent in the single channel current-voltage (*I-V*) relation of DRK1, a result consistent with the outward rectification in the instantaneous *I-V* curve obtained from macroscopic current recordings (*10*). By contrast, no curvature was apparent for DRK-NGK or NGK2, and the extrapolated reversal potential from the single channel *I-V* relation agreed with that expected for a K^+-selective channel.

TEA blocked the chimeric channel in a manner that mimicked TEA blockade of NGK2 and was different from TEA blockade of DRK1. Extracellular TEA at 3.0 mM produced a weak blockade of DRK1 whole-cell currents, a strong blockade of NGK2 currents, and a strong blockade of DRK-NGK currents. By contrast, intracellular TEA at 0.3 mM produced a strong blockade of DRK1 currents, a weak blockade of NGK2 currents, and a weak blockade of DRK-NGK currents (Fig. 3). The differences among the concentration-response curves for extracellular and intracellular TEA blockade of DRK1, NGK2, and DRK-NGK are shown in Fig. 4. Whereas the internal TEA blockade of the chimeric channel was indistinguishable from that for NGK2, the concentration-response curve for external blockade appeared to be intermediate between that of DRK1 and NGK2.

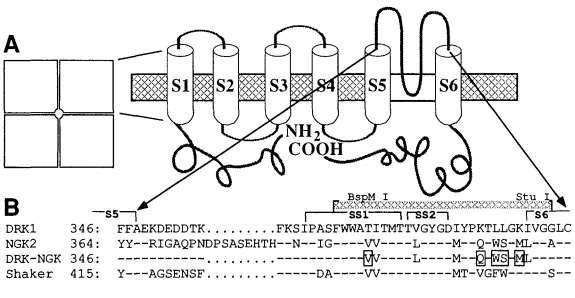

Fig. 1. Construction of a chimeric K^+ channel. (**A**) Model of the topography of a voltage-gated K^+ channel. On the left are four identical subunits arranged about a central pore. On the right is a single subunit with its six putative transmembrane segments and their connecting loops. The loop between S5 and S6 is placed in the membrane to explain the results obtained in this paper. (**B**) Comparison among DRK1, NGK2, the DRK-NGK, and Shaker K^+ channels of the amino acid sequences in the S5-S6 loop. The dashes represent residues identical to DRK1. The dots represent interruptions that maintain the alignment with NGK2. The numbers apply to the first residue in each of the aligned sequences. The cross-hatched bar between the BspM I and Stu I restriction sites indicates the extent of the restriction fragment in DRK1 that was replaced. SS1 and SS2 are two short segments thought to span part of the membrane (*5*). The boxed residues in the chimeric segment are nonconservative differences between NGK2 and DRK1.

H. A. Hartmann, J. A. Drewe, M. Taglialatela, R. H. Joho, A. M. Brown, Department of Molecular Physiology and Biophysics, Baylor College of Medicine, One Baylor Plaza, Houston, TX 77030.
G. E. Kirsch, Departments of Molecular Physiology and Biophysics and Anesthesiology, Baylor College of Medicine, One Baylor Plaza, Houston, TX 77030.